Development 129, 3367-3379 (2002)
Printed in Great Britain © The Company of Biologists Limited 2002
DEV9842



# *unc-53* controls longitudinal migration in *C. elegans*

**Eve Stringham[1,*,§], Nathalie Pujol[1,†,§,¶], Joel Vandekerckhove[1] and Thierry Bogaert[1,2,‡]**

[1]Department of Biochemistry, Ghent University – Flanders Interuniversity Institute for Biotechnology (VIB09), Gent 9000, Belgium
[2]Singapore Institute of Molecular and Cell Biology, Kent Ridge Crescent, Singapore, and Medical Research Council Laboratory of Molecular Biology, Cambridge, CB2 2QH, UK

*Present address: Department of Biology, Trinity Western University, 7600 Glover Road, Langley, BC V2Y 1Y1, Canada

†Present address: Centre d'Immunologie de Marseille-Luminy, CNRS/INSERM/Université de la Méditerranée, Luminy Case 906, 13288 Marseille Cedex 9, France

‡Present address: Devgen N.V., Technologiepark 9, Blok DF1.60.14, 9052 Zwijnaarde, Belgium

§These two authors contributed equally to this work

¶Author for correspondence (e-mail: pujol@ciml.univ-mrs.fr)

*Accepted 29 April 2002*

## SUMMARY

**Cell migration and outgrowth are thought to be based on analogous mechanisms that require repeated cycles of process extension, reading and integration of multiple directional signals, followed by stabilisation in a preferred direction, and renewed extension. We have characterised a *C. elegans* gene, *unc-53*, that appears to act cell autonomously in the migration and outgrowth of muscles, axons and excretory canals. Abrogation of *unc-53* function disrupts anteroposterior outgrowth in those cells that normally express the gene. Conversely, overexpression of *unc-53* in bodywall muscles leads to exaggerated outgrowth. UNC-53 is a novel protein conserved in vertebrates that contains putative SH3- and actin-binding sites. *unc-53* interacts genetically with *sem-5* and we demonstrated a direct interaction in vitro between UNC-53 and the SH2-SH3 adaptor protein SEM-5/GRB2. Thus, *unc-53* is involved in longitudinal navigation and might act by linking extracellular guidance cues to the intracellular cytoskeleton.**

Key words: Cell migration, Axonal guidance, Growth cone steering, Cytoskeleton, *C. elegans*

## INTRODUCTION

The development of higher organisms involves the movement of cells and the extension of cellular processes, such as axons, along complex pathways to defined destinations. Cell migrations and the outgrowth of cellular processes appear to be driven by common mechanisms that have been conserved through evolution. For both, in addition to a general non-directional motility, there is an element of pathfinding, which is associated with the capacity to respond to repulsive and attractive cues from multiple directions (Chisholm and Tessier-Lavigne, 1999; Tessier-Lavigne and Goodman, 1996). The mechanisms by which guidance cues are interpreted, to produce organised rearrangements of the cytoskeleton and hence directional movement are not fully understood.

The nematode *C. elegans* has proved to be an extremely useful genetic model with which to dissect the molecular basis of long-range migrations (Branda and Stern, 2000), especially those associated with the growth of axons along the dorsoventral axis. Not only have guidance cues and their receptors been identified, such as the Netrin UNC-6 and its receptors UNC-5 and UNC-40 (Hedgecock and Norris, 1997), but insights have also been obtained into the complex interplay between signalling pathways. For example, it has been shown that expression of SAX-3 (the worm Robo homologue) and UNC-40 allows the axon of the laterally situated AVM neurone to grow towards UNC-6 expressed by ventral cord axons and away from the SLT-1 cue originating from dorsal muscle cells (Hao et al., 2001).

Less is known about the anteroposterior (AP) migrations of either axons or cells. One of the better characterised examples is that of the anterior migration of the hermaphrodite sex myoblasts (Branda and Stern, 2000). During their journey to the position of the future vulva, they are subject to a gonad-dependent attraction. The attractive cue is EGL-17/FGF, which mediates its effect via EGL-15/FGFR and a downstream signalling pathway that passes through the GRB2 adapter homologue SEM-5. Several other genes, which also function in axon guidance, are known to impinge on the sex myoblast EGL-17 pathway. Their corresponding proteins, UNC-51 (a serine/threonine kinase), its interactor UNC-14 (Ogura et al., 1997), UNC-44 (an ankyrin) (Otsuka et al., 1995), UNC-33 (a protein related to collapsin-response-mediator protein) (Li et al., 1992) and UNC-34, are believed to be localised to the cytoplasm in the sex myoblasts and to act together to transduce the EGL-17 signal (Branda and Stern, 2000). The sex myoblasts are also subject to a gonad-independent attraction that, in addition to *sem-5*, requires the activity of *unc-53*, *unc-71* and *unc-73* (Chen et al., 1997). All of these *unc* genes have been linked to multiple guidance phenotypes, including defects in axon outgrowth or fasciculation (Hedgecock et al., 1987; McIntire et al., 1992; Siddiqui, 1990). While the identity of

*unc-71* has yet to be reported, UNC-73 and its fly homologue TRIO are guanine nucleotide exchange factors (GEFs) that have been shown to regulate Rho GTPases and thereby actin cytoskeleton dynamics (Lin and Greenberg, 2000; Steven et al., 1998). The receptor for this pathway is currently unknown, and until now the role of *unc-53* was unclear. *unc-53* mutants also display premature arrest of the excretory canals (Hedgecock et al., 1987) and of the axons of the mechanosensory neurones (Hekimi and Kershaw, 1993), suggesting that it has a specific role in AP guidance.

We describe the isolation of an additional allele of *unc-53* and the detailed characterisation of the role of *unc-53* in AP axonal and cell migration. We show that the gene encodes a novel protein with several conserved domains associated with signal transduction and actin binding, and that UNC-53 is capable of interacting directly with the adapter protein SEM-5. We show that *unc-53* is expressed in those cells that require its function. Furthermore, we demonstrate that overexpression of *unc-53* results in exaggerated cellular outgrowth. Our results clearly define a role for *unc-53* in AP migration and raise the possibility that UNC-53 acts cell autonomously to integrate multiple directional cues.

## MATERIALS AND METHODS

### Strains

All strains, including the wild type N2 Bristol, those containing the *unc-53* alleles *e2432, e404* (Brenner, 1974), *n152* (Trent et al., 1983), and the deficiencies *mnDf90* (SP756), *mnDf87* (SP753), *mnDf87/mIn1*[*dpy-10(e128);mIs14(myo-2*::GFP)] (CZ1989) and *mnDf77* (SP705), were grown and maintained at 20°C as described previously (Brenner, 1974). The new EMS-induced allele *e2432* was isolated in a screen using Nomarski (DIC) and polarised microscopy for mutants with specific attachment or pattern defects in a subset of the male sex muscles but without defects in body wall muscle pattern or myofilament organisation. The *e2432* allele was mapped to the left arm of chromosome II and was found not to complement *unc-53(e404)*. Transgenic arrays were generated in a wild-type or mutant background using standard techniques (Mello et al., 1991). Transgenic animals were identified by the dominant Roller phenotype conferred by co-injected plasmid pRF4 (that contains *rol-6(su1006)* DNA).

Transgenic strains made for this study are the following:

UG1 *unc-53(n152);bgEx1* [T28D2;pRF4]
UG191 *unc-53(n152);bgEx39* [T28D2;pNP3;pRF4]
UG21 *unc-53(e2432);bgEx9* [S4;pRF4]
UG54 *unc-53(e2432);bgEx12* [S4;pRF4]
UG83 *unc-53(e2432);bgEx16* [S4;pRF4]
UG13 *wt;bgEx3* [pNP3;pRF4]
UG14 *wt;bgEx4* [pNP3;pRF4]
UG17 *unc-53(n152);bgEx3* [pNP3;pRF4]
UG18 *unc-53(e2432);bgEx3* [pNP3;pRF4]
UG38 *wt;bgEx17* [pNP3;pNP8;pRF4]
UG39 *wt;bgEx18* [pNP3;pNP8;pRF4]
UG41 *unc-53(n152);bgEx18* [pNP3;pNP8;pRF4]
UG174 *unc-53(n152);bgEx24* [pNP3;pNP8;pRF4]
UG175 *unc-53(n152);bgEx25* [pNP3;pNP8;pRF4]
UG176 *unc-53(n152);bgEx26* [pNP3;pNP8;pRF4]
UG177 *unc-53(n152);bgEx27* [pNP3;pNP8;pRF4]
UG51 *wt;bgEx10* [pNP10;pRF4]
UG52 *wt;bgEx11* [pNP10;pRF4]
UG53 *unc-53(n152);bgEx10* [pNP10;pRF4]
UG62 *unc-53(n152);bgEx20* [pNP9;pNP10;pRF4]
UG63 *unc-53(n152);bgEx22* [pNP9;pNP10;pRF4]
UG42 *wt;bgEx21* [pNP21;pRF4]
UG85 *unc-53(n152);bgEx21* [pNP21;pRF4]
UG186 *unc-53(n152);bgEx34* [pNP24;pNP21;pRF4]
UG187 *unc-53(n152);bgEx35* [pNP24;pNP21;pRF4]
UG188 *unc-53(n152);bgEx36* [pNP24;pNP21;pRF4]
UG189 *unc-53(n152);bgEx37* [pNP24;pNP21;pRF4]
UG190 *unc-53(n152);bgEx38* [pNP24;pNP21;pRF4]
UG100 *wt;bgEx48* [pTB113;pRF4]
UG101 *wt;bgEx49* [pTB113;pRF4]
UG102 *wt;bgEx50* [pTB113;pRF4]
UG103 *wt;bgEx51* [pPD93.48;pRF4]
UG104 *wt;bgEx52* [pPD93.48;pRF4]

### Analysis of *unc-53* phenotypes

To visualise the sex muscle phenotype of *unc-53* mutants, young adults were mounted on 2% agarose pads containing 0.2% phenoxypropanol as described (Sulston and Horvitz, 1981) and observed using polarised light (with a Brace Kohler compensator) or DIC microscopy. In addition, adults were fixed, incubated with FITC-coupled phalloidin and mounted for fluorescence microscopy, as described (Goh and Bogaert, 1991). The stop points of the excretory canals were recorded in young adult hermaphrodites by DIC microscopy. Egg-laying was assayed by directly counting the number of progeny. As *unc-53* hermaphrodites are not sterile, sick or starved, this accurately reflects defects in egg-laying (Trent et al., 1983). The effect of the different reporter GFP constructs (pAB::GFP, pA::GFP and pB::GFP) was assayed in the wild-type and *n152* background and found not to influence the number of progeny (results not shown). The ALN and PLN axons were visualised in young adult hermaphrodites in transgenic strains carrying the pA::GFP reporter construct. The stop points of these axons were scored with reference to the position of the vulva and the anus.

### Mapping and cloning of *unc-53*

*unc-53(e2432)* was mapped by three-factor crosses between *unc-4* and *sqt-1*, 0.23 map units to the left of *sqt-1*, and relative to three deficiencies in the region. *mnDf87* and *mnDf90* do not complement *unc-53(e2432)*, whereas *mnDf77* does. Southern blots of genomic DNA from the wild-type and deficiency strains were probed with cosmids throughout the region. Cosmid K02F7 is deleted in *mnDf90* but not deleted in *mnDf87* and *mnDf77*, thus identifying a leftmost location for *unc-53*. The genomic region covered by cosmids W10G4, T08D11 and F33G3 are not deleted in *mnDf77* but are deleted in *mnDf87* and *mnDf90*. Cosmid K04H9 is deleted in *mnDf77* and identifies a rightmost location for the gene. Further mapping of *unc-53* relative to RFLPs placed *unc-53* in an interval of 80 kb. Among cosmids from this region tested for their capacity to rescue *unc-53(n152)*, T28D2 was found to rescue the Unc and Egl phenotypes. A genomic library of N2 in lambda2001 (the kind gift of A. Coulson) was screened with T28D2 and flanking overlapping cosmids. Lambda clone S4 carrying a 16 kb insert was shown to partially rescue *unc-53(n152)*. Deletions in alleles *n152* and *e2432* were identified by Southern analysis and confirmed by sequencing. The allele *n152* corresponds to a deletion of 319 bp from the alternative exon 18 to intron 19, while *e2432* carries a deletion of 375 bp from exon 12 to intron 13, giving the breakpoint sequences CCCCACGAAGAT-ctaattttcaac and TACGATGTTCTT-aaacttttttctt, respectively.

### Characterisation of *unc-53* cDNAs

The 9 kb *Xho*I genomic fragment from the S4 phage was cloned into pBKS to give X16. Using this *Xho*I restriction fragment as a probe, cDNA clones CE5, CE6 and CE7 were isolated from a Lambda MGU1 cDNA library (a gift from R. Barstead). The insert of the largest clone, CE5, was entirely sequenced. It contains part of the SL1 trans-spliced leader sequence (Krause and Hirsh, 1987), a 5′ UTR of 42 bp and the entire coding sequence of *unc-53*, corresponding to 23 exons (GB#AF504312). To confirm the 5′ end of the *unc-53* transcript,

we performed nested PCR on L2 stage random primed cDNA (a gift from D. Zarkower), between antisense primers tab2 (agatgtggaatgcatgctta) and tab14r (gggaaccttccgtcgatgat) in exon 9 and the SL1 primer. These PCRs yielded six classes of PCR fragments that were subcloned and sequenced. Comparison with the genomic sequence indicated that SL1 was alternatively trans-spliced to sites 3′ of the splice site seen in CE5, at downstream intron-exon boundaries, as represented in Fig. 3A. Similar PCR reactions with an SL2 primer produced no reaction products. The available sequence for cDNA yk25d6 (GB#D35780) suggests that an alternatively spliced transcript, which lacks exons 17 and 18 also exists. A 3′ UTR of 216 bp is found in several cDNAs (yk25d6, yk244c7, yk398f6, yk442c6, yk544g8 and yk597h4) with the standard AATAAA polyadenylation signal. Note that the exons 1, 2, 3, 7, 17 and 18 (Fig. 3A) were not present in the predicted protein F45E10.1 (GB#CAA87784). Northern blot analysis identifies a major transcript of around 5.0 kb and at least two smaller transcripts that are expressed in L2, L4 and adult worms (D. Zarkower and T. B., unpublished).

### *unc-53*::GFP constructs

To monitor *unc-53* expression, several translational *unc-53*::GFP fusions were constructed. pAB::GFP (pNP3) contains 6.2 kb of genomic sequence from the *Xho*I site in exon 5 to the *Spl*I site in exon 13. To construct it, a PCR amplicon, with flanking *Spl*I sites, corresponding to the GFP-coding region and poly A tail of *unc-54* from pPD95.75 (a gift from A. Fire) was inserted into the unique *Spl*I site of X16 (see above). pA::GFP (pNP10) contains 2.8 kb of genomic sequence from the *Xho*I site in exon 5 to the *Nhe*I site in exon 8 fused to the GFP coding region and poly A tail of *unc-54* from pPD95.75. pB::GFP (pNP21) contains 3.4 kb of genomic sequence from the *Nhe*I site in exon 13 to the *Spl*I site in exon 13 fused to the GFP-coding sequence; it was generated by deleting the *Apa*I-*Nhe*I fragment from pNP3. Further details of the constructs are available upon request. Several independent strains were generated in a wild-type or *unc-53(n152 or e2432)* background with the constructs pAB::GFP (UG13, UG14, UG17, UG18), pA::GFP (UG51, UG52, UG53) and pB::GFP (UG42, UG85).

### Rescuing minigenes constructs

Fragments derived from the three constructs used to monitor GFP expression were used to construct three equivalent minigenes to test the rescue of the different phenotypes. pAB::*unc-53* (pNP8), pA::*unc-53* (pNP9) and pB::*unc-53* (pNP24) contain the same upstream genomic region as pAB::GFP, pA::GFP and pB::GFP, respectively, but fused to a *unc-53* cDNA contained in pTB72 (derived from CE5, see below) at the *Spl*I, *Bst*XI or *Spl*I sites, respectively (Fig. 3). Further details of the constructs are available upon request. Several independent strains were generated in an *unc-53 (n152)* background with the constructs pAB::*unc-53* (UG41, UG174, UG175, UG176 and UG177), pA::*unc-53* (UG62 and UG63) and pB::*unc-53* (UG186, UG187, UG188 UG189 and UG190).

### Overexpression constructs

To express *unc-53* in bodywall muscle, we cloned an *Xba*I-*Kpn*I fragment derived from CE5 into the *Nhe*I-*Kpn*I sites of the expression vector pPD30.38 (a gift from A. Fire), which contains the myosin heavy chain *unc-54* promoter, to obtain p*unc-54::unc-53* (pTB113). This construction contains the entire *unc-53* CE5 cDNA, starting from the first initiation codon and including the *unc-53* stop codon and 60 bp of the 3′ UTR, but lacks the 5′ UTR and the SL1 leader. Three independent p*unc-54::unc-53*-containing strains (UG100, UG101 and UG102) were generated in a wild-type background. The presence of the transgene was associated with a marked degree of lethality. To evaluate this, ten healthy adult hermaphrodite transgenic worms were allowed to lay eggs for 48 hours at 20°C. The number of mutant larvae, unhatched embryos and the total number of transgenic progeny was counted. Lethality was never observed in two p*unc-54*::GFP (pPD93.48) control strains (UG103 and UG104), also generated in a wild-type background.

### Expression constructs

To optimise in vitro translational initiation at the first methionine, a mammalian KOZAK consensus sequence was engineered upstream of the *unc-53* initiation codon by PCR amplification with BG03 (ataagaatgcggccgccgccatgacgacgtcaaatgtagaattgata) that contains the KOZAK consensus sequence and a *Not*I restriction site and BG02 (cgcggatcctcaaaccgcgggtggcataatggatg) that contains a *Bam*HI site. The digested amplicon, which contains the first 139 codons of *unc-53*, was then fused to the complementary fragment of the *unc-53* cDNA, derived from CE5, to reconstitute the entire coding sequence. This was then cloned as a 5.1 kb *Not*I-*Apa*I cassette in the mammalian expression vector pCDNA3 (Invitrogen) to generate plasmid pTB72. The construct pTB50 contains a C-terminal deletion of the last 71 codons (UNC-53Δ71C) cloned into the *Not*I and *Apa*I sites of pBluescript II-KS.

A convenient *Nde*I cloning site was generated immediately upstream of the *unc-53* initiation codon, by PCR amplification with BG01 (ggaattccaaccatatgacgacgtcaaatgtagaattgaata) and BG02. The *Nde*I-*Bam*HI-digested amplicon, which contains the first 139 codons of *unc-53*, was then cloned into the prokaryotic expression vector pRK172 (McLeod et al., 1987) to generate construct pTB57. pTB61 contains the 5′ PCR amplicon-derived end of the *unc-53* cDNA from pTB57 joined at the level of the common *Sac*II site to the truncated 3′ end of the cDNA present in pTB50 (UNC-53Δ71C). Further details of the constructs are available upon request.

### Generation of an anti-UNC-53 monoclonal antibody, mAb 16-48-2

A *Nde*I-*Eco*RI fragment of the *unc-53* cDNA CE5 (corresponding to amino acids 1043 to 1465) was subcloned in pRK172 to generate pTB66 and expressed in *E. coli* strain BL21DE3. The corresponding recombinant fusion protein was purified over a DEAE column equilibrated in 8 M urea, emulsified in complete Freund's adjuvant and injected in Lou rats (Ausubel et al., 1993). All derived antisera were shown to be active at titres of 1:30,000 on western blots of extracts from bacteria expressing recombinant UNC-53. Rat-mouse hybridomas were prepared as described (Ausubel et al., 1993) and a hybridoma cell line producing a monoclonal antibody to UNC-53, designated MAb 16-48-2 was identified using the western blot assay. The specificity of the antibody was confirmed by immunostaining of UNC-53 in wild-type embryos, the absence of reactivity in the *n152* deletion mutant and restoration of the signal in transgenic overexpression experiments. MAb 16-48-2 failed to detect antigen of the correct size on western blots of total nematode proteins or proteins fractionated by progressive extraction with detergents, urea and SDS.

### Immunostaining and microscopy

To detect UNC-53, embryos were washed, freeze-cracked, fixed and permeabilised as previously described (Goh and Bogaert, 1991). Fixed specimens were incubated overnight in primary antibody solution (1:200 dilution of MAb 16-48-2), washed three times in TBS-Tween (0.1%), and incubated for between 1 and 16 hours in a secondary antibody solution (1:200 dilution of Cy3-conjugated donkey anti-mouse; Jackson Laboratories). The nematodes were washed three times in TBS-Tween and mounted in 2% propylgallate, 80% glycerol (pH 8.0) or in a commercially available mounting medium (Vectashield, Vector Laboratories) and observed using a Zeiss axiophot.

### Immunoprecipitations and SEM-5/GRB2 binding experiments

UNC-53Δ71C protein, labelled radioactively with $^{35}S$, was produced by in vitro translation in rabbit reticulocyte lysates from the construct pTB50. It was immunoprecipitated with the MAb 16-48-2 under

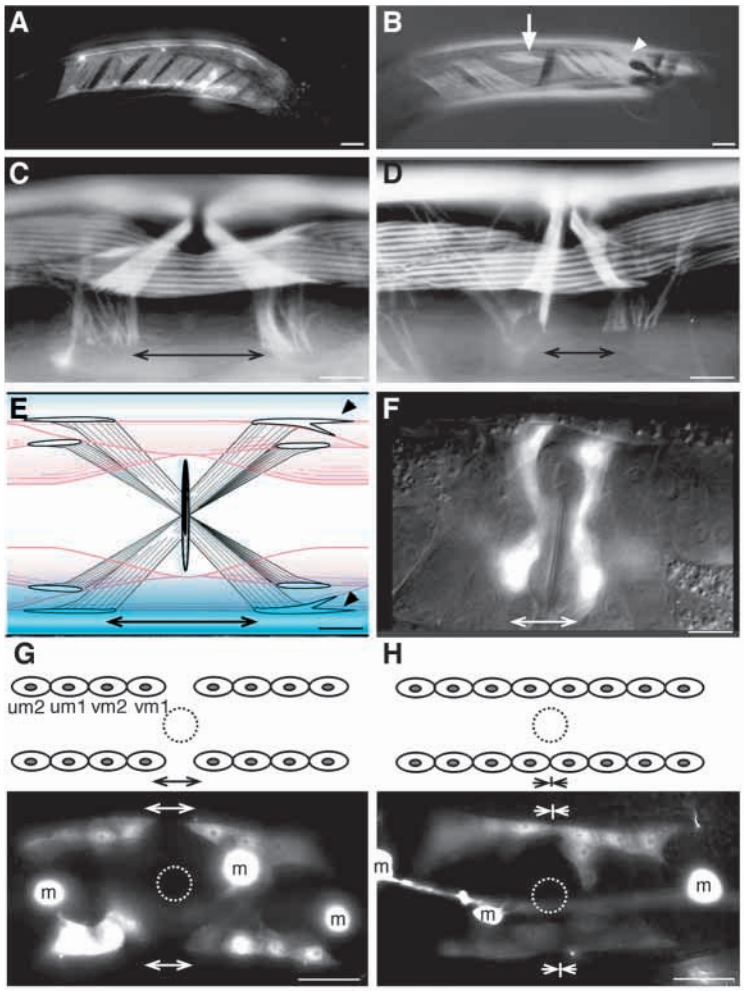


**Fig. 1.** *unc-53* sex muscle phenotypes. (A,B) Male sex muscles; lateral view. (A) Wild type with a pAB::GFP reporter revealing the diagonal muscles. (B) In the *unc-53(e2432)* mutant, which is stained with phalloidin-FITC, one diagonal muscle is shorter than normal and is attached in a dorsal position (arrow); the spicule retractor muscles are also abnormally short (arrowhead). (C-F) Hermaphrodite sex muscles. (C,D) Lateral view of wild-type (C) or *unc-53* (D) vulval muscles (vms) with phalloidin-FITC staining. The distance between the anterior and posterior vm1 cells is reduced in the mutant as indicated by the double-headed arrows. (E) A schematic ventral view of the wild-type vulval muscles, bodywall cells are in red, seam cells in blue. The feet-like structures extending from the base of the four vm1 and four vm2 muscles are shown (arrowhead). (F) Ventral view of the four vm1 in *unc-53(n152)* revealed with a pAB::GFP reporter. No feet-like structures are visible, and the vm do not attach at their normal position. (G,H) Ventral view of the sex myoblasts during their division and migration in the wild-type (G) and *unc-53(n152)* (H) worms. Top, idealised schema; bottom, fluorescent images of worms expressing the pAB::GFP reporter. In the mutant, no longitudinal migration is observed and the distance (indicated by the arrows) between the anterior and posterior set of sex myoblasts is eliminated; they are all grouped around the future vulva (dotted circle) in the mutant. The bright round cells are motoneurones (m) in a higher plane of focus. Scale bars: 10 μm.

denaturing conditions (0.4% SDS, 2.0% Triton X-100) for 1 hour at room temperature, then incubated with protein G sepharose for 2 hours at room temperature. The beads were washed three times with PBS and the bound products analysed by SDS-PAGE and fluorography. As a control, a reaction without MAb 16-48-2 was treated identically. For a GST pull-down assay, the same protein was incubated with glutathione resin bound to GST (glutathione-S-transferase) protein or to a GST-SEM-5 fusion protein for 1 hour at 20°C. After incubation, the beads were washed four times with phosphate-buffered saline (PBS)/Triton X-100 (0.2%) and the bound proteins analysed by SDS-PAGE and fluorography. For the western overlays, UNC-53Δ71C protein was expressed in *E. coli* from the pTB61 construct and incubated with either GST or GST-GRB2 proteins that had been biotinylated. The blots were revealed using an alkaline phosphatase-linked anti-streptavidin antibody and chromogenic substrate following standard procedures. The SEM-5 and GRB2 GST fusion constructs (Lowenstein et al., 1992; Stern et al., 1993) were a kind gift from M. Stern.

## RESULTS

### Isolation of a new *unc-53* allele

In a search for *C. elegans* genes involved in specific aspects of cell adhesion or migration, we screened for mutants with defects in the sex muscles but without defects in the body-wall muscles, myofilament organisation or overall anatomy. The sex muscles bridge the hypodermis and gonads, develop post-embryonically and are not required for viability. From this screen, the allele *e2432* was isolated. Upon further characterisation, it was found to be an allele of *unc-53*. Several *unc-53* alleles have been previously identified. The *unc-53(e404)* allele was isolated by Brenner based on its uncoordinated (Unc) phenotype, being incapable of correct reverse locomotion (Brenner, 1974). Homozygous mutants are healthy if slightly 'dumpyish' in size, and males present a defect in mating (Hodgkin, 1983). In a screen for egg-laying defective (Egl) mutants, the *unc-53* allele *n152* was identified (Trent et al., 1983). A further screen, for genetic enhancers of sex myoblast migration defects in a sensitised *sem-5* background, yielded three additional *unc-53* alleles, *ay10*, *ay11* and *ay62* (Chen et al., 1997). Consistent with the results of the previous screens, homozygous *unc-53(e2432)* mutants are Unc, Egl and exhibit poor male mating.

### Only two types of sex muscles are defective in *unc-53* males

In the male, there are 41 sex-specific muscles that develop post-embryonically and function during mating. In the wild type, the 15 diagonal muscles are distributed along the posterior body parallel to each other, seven on the left and eight on the right, and contribute to the characteristic ventral arching of the male tail (Sulston et al., 1980) (Fig. 1A). In *unc-53* mutants, the diagonal muscles are frequently not parallel to one another, or have a dorsal attachment point that is more ventrally positioned than in wild type (Fig. 1B). All *unc-53*(*n152*) homozygous males display at least one defective muscle.

During copulation, two spicules are inserted through the hermaphrodite vulva. In the wild type, each spicule is attached at its proximal end to two associated protractor and retractor muscles. The retractor muscles are attached anteriorly to the body wall (Sulston et al., 1980). In *unc-53* mutants, the

retractor muscles are shorter than in wild-type worms. The attachment point to the body wall is shifted posteriorly and frequently more ventrally to the edge between the seam and body wall muscles (Fig. 1B), while their attachment to the spicules is normal. In addition, in *unc-53* mutants, the protractor muscles sometimes extend processes onto the attachment point of the retractor muscles on the hypodermis, suggesting that the defect is not in these attachment points, but rather in the extension of the muscles towards their normal point of attachment. Moreover, in *unc-53* males, the fan and pattern of the rays are normal, suggesting that the sex muscle defect is not likely to be due to generalised defects in the hypodermis. However, the observed defects in muscles required for copulation explain the observed mating phenotype of *unc-53* males.

### Longitudinal migration of the developing sex myoblasts is affected in the *unc-53* hermaphrodite

In the hermaphrodite, the vulval muscles are a set of four pairs of cells arranged symmetrically in a cross-pattern around the vulval slit (Fig. 1E). Their simultaneous contraction enables the vulva to open and the eggs to be laid. Each pair consists of one vm1 and one vm2 muscle cell (Sulston and Horvitz, 1977). The vm muscles attach proximally to the vulva and distally to the hypodermis (White et al., 1986), at the dorsal margin of the ventral body wall muscle cells for vm1, or in between the two ventral body wall muscle cells for vm2 (Fig. 1C,E). In all *unc-53(n152)* mutants, the vm1 and vm2 muscles are shorter than in wild type. Their proximal attachment is normal, but their distal attachment is abnormal, being in an apparently random position closer to the vulva (Fig. 1D).

To understand the origin of this phenotype, sex muscle development was examined throughout the L4 stage using a GFP reporter gene pAB::GFP (see below), which is expressed in the sex myoblasts and their descendants, and permits the visualisation of cell shape and growth cone spikes not visible by DIC microscopy. In wild-type hermaphrodites, after their migration to the position of the future vulva, the two sex myoblasts divide three times, giving rise to two groups of cells on each side of the vulva: the future vm1 and vm2, and the future uterine muscles um1 and um2 (Sulston and Horvitz, 1977). During division, these groups of myoblasts migrate along the longitudinal axis away from the vulva, leading to four clearly separate groups of cells (Fig. 1G). This migration fails to occur in *unc-53(n152)* mutants, resulting in a cluster of myoblasts that flanks the vulva too closely on either side of the animal (Fig. 1H). The vulval myoblasts then send cellular extensions ventrally to attach to the vulva, while remaining attached at the other end to the hypodermis. This ventral extension is wild type in *unc-53* mutants. Concomitantly, the vulval myoblasts extend thin distal growth cone extensions longitudinally along the seam. These feet-like structures may serve to further anchor the muscles to the hypodermis (Fig. 1E and see Fig. 4J). In *unc-53* mutants, these feet-like structures are not made, and the muscles only attach over the width of the myofilaments, yielding rounded muscle attachments (Fig. 1F). Occasionally, the vm1 muscles do not remain connected to the seam and attach more ventrally in between the body wall muscles, at the site left vacant by the vm2 muscles. These observations thus reveal a specific problem in AP migration and extension of the sex muscles.

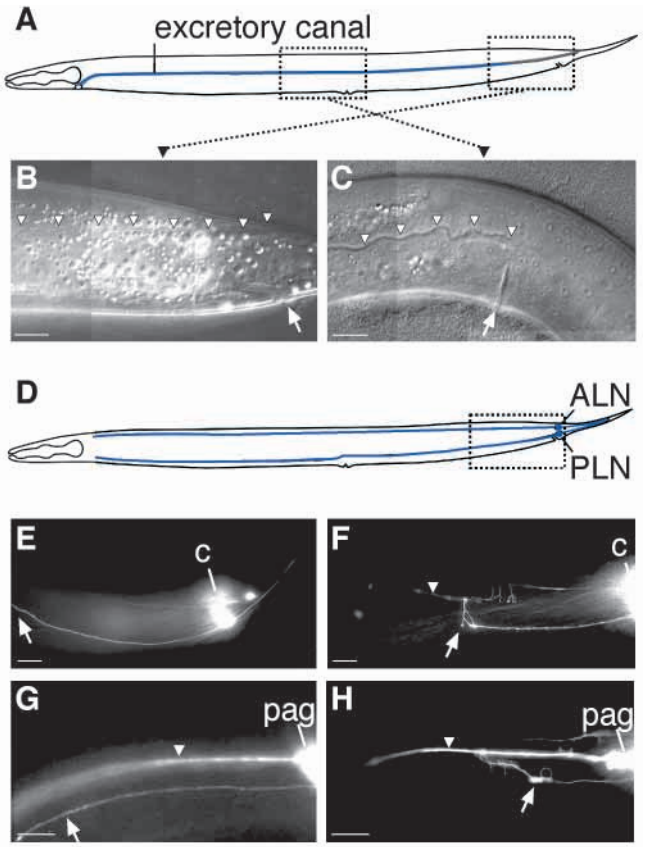


**Fig. 2.** Longitudinal migration defects in *unc-53* mutants. (A) The wild-type excretory canal. Two posterior canals extend from the excretory cell on each side along the lateral cord from the head to the tail. The boxes show the regions represented in B,C. These are DIC photomicrographs of adult worms showing the trajectory of the excretory canal (arrowheads). (B) In the wild type, the canal stops at the level of the anus (arrow). (C) An *unc-53(n152)* mutant, with a canal that stops at the level of the vulva (arrow). (D) The wild-type ALN and PLN projections. ALN and PLN send anteriorly directed axons up to the head along the sublateral dorsal and ventral cords, respectively. The box shows the region represented in E-H. These are fluorescence photomicrographs of adult wild-type (E,G) and *unc-53(n152)* mutant (F,H) worms expressing a pA::GFP reporter construct, showing the trajectory of an ALN (E,F) or PLN (G,H) axon (arrows). (F) The ALN axon has stopped its anterior outgrowth before the mid-body and sends several dorsal branches directly to the dorsal cord (arrowhead). (H) The PLN axon has stopped its anterior outgrowth before the mid-body and sends several dorsal branches to the ventral cord (arrowhead). c, cell body; pag, pre-anal ganglion. Scale bars: 10 μm.

This cellular defect explains the observed egg-laying defective phenotype of *unc-53* mutants. All adult homozygous *n152* and *e2432* hermaphrodites become bloated with late stage embryos that hatch internally and eventually kill the mother, the so-called ‘bag of worms’ phenotype. The Egl phenotype was equally strong for *unc-53(n152)* mutants as for heterozygous *n152/mnDf87* worms (see Fig. 5A), suggesting that *n152* is a strong loss-of-function or null allele for this phenotype.

### Further abnormal AP migrations in *unc-53* mutants

The excretory cell in *C. elegans* is a large H-shaped cell whose

**Table 1. Cells that express *unc-53* reporter constructs in adults are associated with a phenotype in *unc-53* mutants**

| Neurones | | | Muscles and other cells | | |
|---|---|---|---|---|---|
| Cells | Express p*unc-53*::GFP | Require *unc-53* | Cells | Express p*unc-53*::GFP | Require *unc-53* |
| Two ALN | pA | + | Four vulval muscles 1 | pB | + |
| Two PLN | pA | + | Four vulval muscles 2 | pB | + |
| Two PVP | pA | nd | Four uterine muscles 1 | pB | nd |
| Two PVQ | pA | nd | Four uterine muscles 2 | pB | nd |
| Two BDU | pA | nd | Two intestine muscles | pB | + |
| Two PVM | pA | nd | Sphincter muscle | pB | nd |
| Nine DA | pB | +* | 15 diagonal muscles | pB | + |
| 11 AS | pB | +* | Two spicule retractors | pB | + |
| ALA | pB | + | Bodywall muscles | pB | + |
| RID | pB | nd | Excretory cell | pA | + |
| Two PDE | pB | +† | Four VulC cells | pA | nd |
| Two HSN | pB | +‡ | Two PDE socket cells | pA | nd |
| Two ALM | nd | +†,§ | Two AM socket cells | pB | + |
| Two PLM | nd | +†,§ | Two PH socket cells | pB | + |
| M5 | pB | nd | Two distal tip cells | pB | +¶ |

Two promoters, pA and pB, give rise to an expression in different cell types. The promoter pAB which is a fusion of both pA and pB presents an additive pattern of the expression seen with pA and pB.

This list is incomplete as there are several unidentified cells in the head that express pAB*unc-53*::GFP.

*DA and AS motoneurones are involved in backwards movement, which is impaired in *unc-53*. In 46% of *unc-53(n152)* mutants ($n$=65), between one and three of the visible motorneurone commissures failed to join the dorsal cord. Overall, 13% of the visible commissures ($n$=372) were abnormal, and exhibited highly variable phenotypes: some axons stopped prematurely, others turned anteriorly along the lateral cords.

†Hedgecock et al., 1987.

‡Wightman et al., 1997.

§Siddiqui, 1990; Hekimi and Kershaw, 1993.

¶A variable gonad morphology defect was observed rarely in *unc-53(e2432)* homozygotes (T. B., unpublished).

nd, not determined due to the difficulty of observation.

cell body is located ventrally to the posterior bulb of the pharynx in the head of the worm (Sulston and Horvitz, 1977). During the three-fold stage, two processes called canals grow dorsal to the lateral midline, where they bifurcate and extend anteriorly and posteriorly over most of the length of the animal (Nelson et al., 1983). Although the dorsal migration was normal in *unc-53(n152)*, in 83% of mutants, the posterior canals of the excretory cell terminated their AP migration prematurely at the level of the vulva ($n$=100; Fig. 2A and see Fig. 5C). In *n152/mnDf87* heterozygotes, 96% of the canals stopped at the same level ($n$=52), suggesting that *n152* is a strong loss-of-function allele for this phenotype as well (Fig. 5C). In worms homozygous for the alleles *e2432* and *e404*, the majority of canals progressed further past the vulva but terminated before the tail (T. B. and I. Maillet, unpublished) (Hedgecock et al., 1987). Frequently, the canal processes in *unc-53* mutants meander and even reverse their path before stopping prematurely. These data suggest that *unc-53* is required for the excretory canal to grow in the correct direction, particularly during its trajectory from the level of the presumptive vulva to the tail.

ALN and PLN are two pairs of neurones located in the tail ganglion. Normally, they send axons anteriorly as far as the head along the sublateral cord (Fig. 2D,E,G). In the mutants, the ALN and PLN axons frequently stopped prematurely (Fig. 2F,H), with 75% and 48% of axons, respectively, failing to reach the mid-body region in *unc-53(n152)* mutants (Fig. 5B). Such premature arrest was associated in the case of the ALN neurones with the appearance of dorsally directed ectopic branches that joined the dorsal cord (Fig. 2F). A similar phenotype was observed for the PLN axon, but in this case, the ectopic branches joined the ventral cord (Fig. 2H). For another anteriorly directed neurone, the PLM, ventral ectopic branching of prematurely arrested axons has previously been reported in *unc-53* mutants (Hekimi and Kershaw, 1993).

*unc-53* might play a minor role in DV migration, as the dorsal outgrowth of the DA and AS motoneurone axons was sometimes abnormal in *unc-53(n152)* mutants (see Table 1). However, ventral migrations of the sex myoblasts and DV outgrowth of excretory canals (see above), mechanosensory neurones (Siddiqui, 1990; Hekimi and Kershaw, 1993), HSN (Wightman et al., 1997) and PDE (N. P., unpublished) are not affected in *unc-53* mutants. Taken together, these results suggest that *unc-53* is required for the navigation of cells and cellular processes along the AP axis.

## *unc-53* encodes a conserved protein of 1583 amino acids

Genetic mapping had previously placed *unc-53* between *bli-1* and *rol-1*, 3 cM to the right of the centre of *LG II* (Brenner, 1974). The position of the gene was further refined by mapping deletion end points and RFLPs (see Materials and Methods). Transformation rescue of *unc-53(n152)* by microinjection of cosmids from the candidate region of the physical map showed that the gene is contained within T28D2 (Fig. 3A and see Fig. 5A,C). The overlapping cosmid C09H10 failed to rescue, while F45E10 partially rescued the Unc and Egl phenotypes, as did the phage S4. The cosmid T28D2 contains a single predicted gene that spans over 16 kb. The generation and sequencing of specific RT-PCR products and cDNAs led to the refinement of this prediction and revealed the *unc-53* locus to be complex. The complete gene is composed of up to 23 exons, ranging in size from 30 bp to 1.5 kb, and covers 31 kb of genomic sequence. Many differently spliced transcripts were identified,

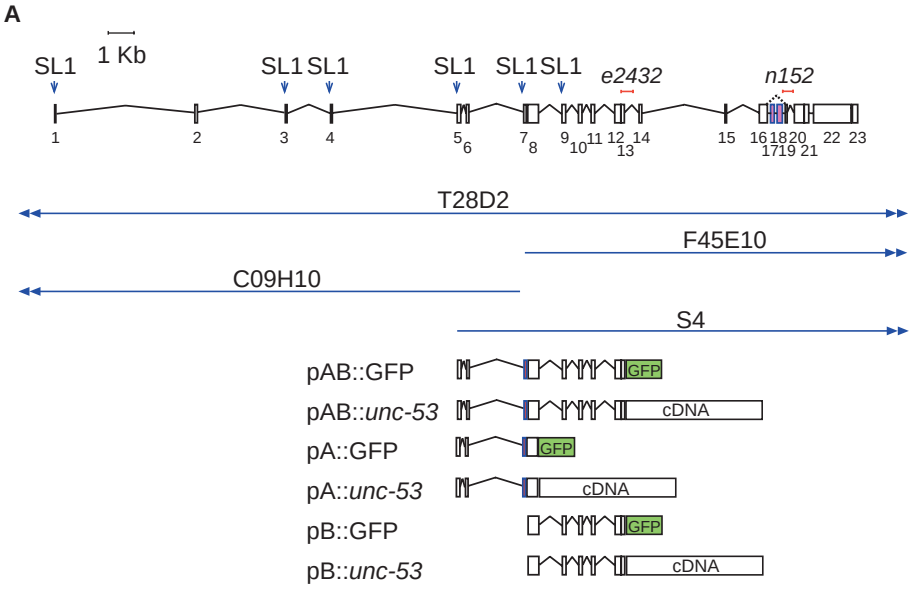


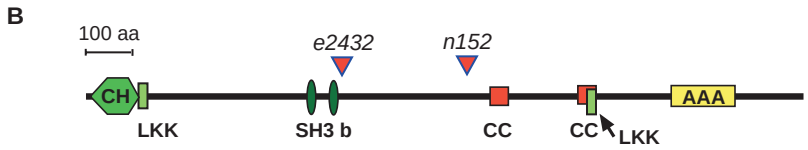


C

**Calponin Homology (CH) domain**

```
Consensus-CH    ALLRWINSLLAEYDGVP-VTNFSSDLKDGVALCKLLNSLSPGSIDKKKVAPPA--LS
CeUNC-53        IYTDWANRHLSKGSLSKSIRDISNDFRDYRLVSQLINVIV--PINEFSPAFTKRLAK
HsNAV2          IYTDWANHYLAKSGHKRLIRDLQQDVTDGVLLAQIIQVVANEKIEDINGCPKNR-SQ
GgDystrophin    TFTKWINAQFAKCG-RRCIEDLFNDFRDGRKLLELLECLTGQKI-----AK-EKGST
Hsα-Actinin     TFTAWCNSHLRKAG-TQ-IENIEEDFRDGLKLMLLLEVISGERL-----AKPERGKM

Consensus-CH    RFKKIENINLALSFAEKLVGKVVLFEPEDLVEGK-KLILGVIWTLI
CeUNC-53        ITSNLDGLETCLDYLKNLGLDCSKLTKTDIDSGNLGAVLQLLFLLS
HsNAV2          MIENIDA---CLNFLAAKGINTQGLSAEEIRNGNLKATLGLFFSLS
GgDystrophin    RVHALNNVNKALQILQRNNVDLVNIGSSDIVDGNHKLTLGLIWNII
Hsα-Actinin     RVHKISNVNKALDFIASKGVKLVSIGAEEIVDGNVKMTLGMIWTII
```

**SH3-binding motif**

```
Position in helix  1  4  7
Consensus          xPhPPhP
CeUNC-53        KKDPPPAVPPRDT
CeUNC-53        TTDVPPLPPLKSV
MmSOS-1         EVPVPPPVPPRRR
MmSOS-1         HLDSPPAIPPRQP
MmSOS-1         HSIAGPPVPPRQS
DmSOS           YRAVPPPLPPRRK
DmSOS           GELSPPPIPPRLN
MmDynamin       APAVPPARPGSRG
RnPI3K-p85      PPRPLPVAPGSSK
RnPI3K-p85      PAPALPPKPPKPT
```

**LKK-binding motif**

```
CeUNC-53        LFLLLSTY-KQKLRQLKKDQKKL
CeUNC-53        TVNVNKL-KTENKQLKKEVDKL
HsNAV2          DSELNEL-RKTIELLKKQNAAA
HsNAV2          REAMNRM-QSEIEKLKAENDRL
Villin          PAAFSALPRWKQQNLKKEKGLF
Dematin         PEEFGKLALWKRNELKKASLF*
Thymosin        LELTDKINNFPSENLKKTETIE
```

**ATP/GTP-binding motif (P-loop)**

```
Consensus       GxxxxGKS
CeUNC-53        LAGATGIGKSKLA
HsNAV2          LSGPSGTGKTYLA
```

**Fig. 3.** Molecular organisation of the *unc-53* gene. (A) The exon-intron structure of the *unc-53* gene. The different SL1 transpliced sites are indicated, as well as the regions deleted in alleles *n152* and *e2432*. Alternatively spliced exons are in pink. The extent of the phage and several cosmid clones are shown. The structure of the different GFP and minigenes constructs is also presented. (B) Structure of UNC-53. UNC-53 contains a calponin homology domain (CH, light green; amino acids 11-109), two proline-rich SH3-binding motifs, (SH3 b, dark green; 487-495 and 537-545), two coiled-coil regions (CC, red; 890-923 and 1078-1113; predicted by COILS at http://www.ch.embnet.org) and an ATPases associated with diverse cellular activities domain (AAA, yellow; 1292-1425) that contains a NTP-binding motif (1300-1307). The positions of the two potential LKK motifs (green, 114-133; 1097-1116) are indicated. Arrowheads mark the positions corresponding to the start of the *e2432* and *n152* deletions. (C) Alignment of the CH domain (PF00307), SH3-, LKK and NTP-binding motifs (PS00017). The Genbank Accession numbers for all the sequences used are: CeUNC-53, AF504312; HsNAV2, AX009326; Hsα-actinin, P12814; GgDystrophin, P11533; MmSOS, Q62245; DmSOS, P26675; MmDynamin, P39053; RnPI3K-p85, Q63787; HsVillin, XP_010866; HsDematin, Q08495; CeThymosin, T32473.

representing both alternative SL1 trans-splicing events and internal splicing of alternative exons (Fig. 3A). Southern analysis revealed the presence of polymorphisms in the T28D2 region of two mutant alleles *n152* and *e2432*, and subsequent sequencing revealed the corresponding molecular alterations. In allele *e2432* a deletion of 374 bp removes part of exon 12, and all of exon 13. Allele *n152* carries a 319 bp deletion, which would be predicted to remove part of alternatively spliced exon 18, and exon 19, thereby introducing a premature stop codon in exon 20.

The largest *unc-53* transcript encodes a putative protein product of 1583 amino acids for which three human

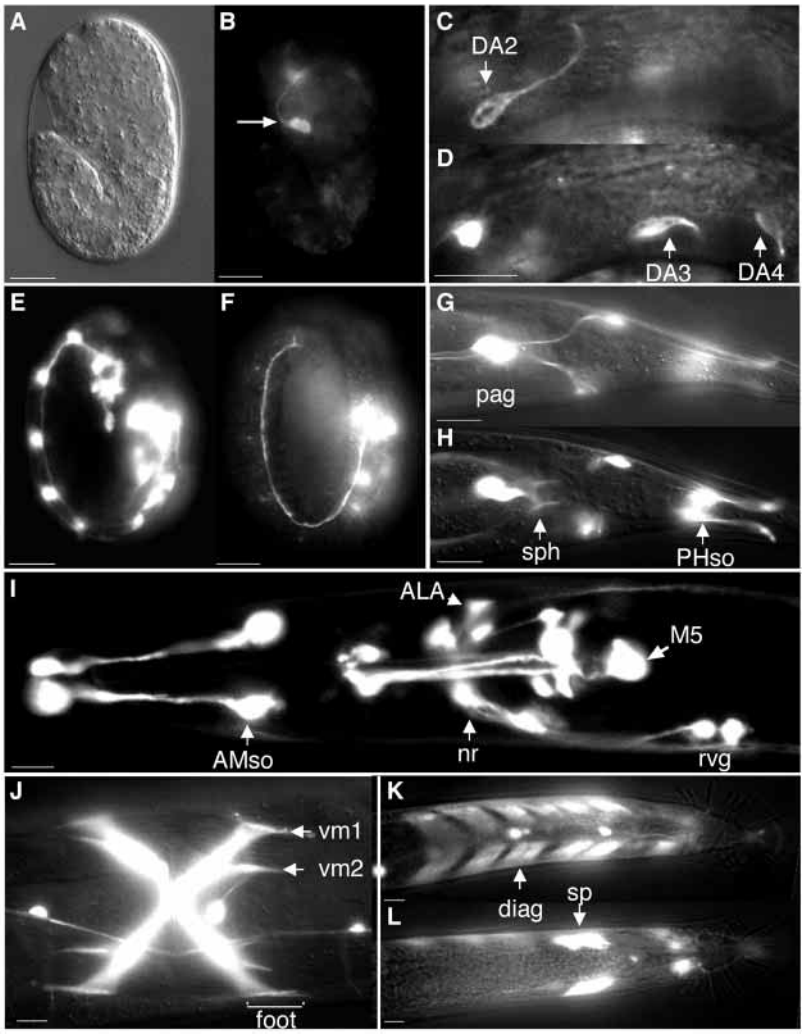


**Fig. 4.** p*unc-53*::GFP expression pattern. DIC (A) and fluorescence images of pAB::GFP expression in transgenic animals (B-H). (A-F) Embryos of successive stages. (A,B) 1.5-fold stage embryo showing a pioneering neurone growing in the head (B, arrow). (C,D) A view between the end of the pharynx and the mid-body of a three-fold stage embryo, showing expression in DA motoneurones pioneering the dorsal cord; C and D are two different focal planes. (E,F) Late three-fold stage embryo: (E) shows the ventral side, (F) the dorsal side, revealing expression in all DA motoneurones and some neurones in head and tail ganglia. (G-L) Adult stage; anterior is towards the left. (G,H) Adult tail, ventral (G) and mid-plane (H) views showing expression in a phasmid socket (PHso), sphincter muscle (sph) and neurones in the preanal ganglion (pag). (I) Adult head showing expression in the amphid socket (AMso), ALA and several neurones in the dorsal, ventral and retrovesicular ganglion (rvg), as well as pharyngeal neurones, including M5. nr, nerve ring. (J) Ventral view of the mid-body showing vulval sex muscles (vm1 and vm2) of an adult hermaphrodite. One of the four foot-like attachments is highlighted. Ventral (K) and dorsal (L) views of the male tail, showing specific expression in diagonal (diag) and spicule retractor (sp) muscles. Scale bars: 10 μm.

homologues have recently been identified (Maes et al., 2002). In terms of sequence, UNC-53 is overall most closely related to human NAV2/RAINB1 (Maes et al., 2002; Merrill et al., 2002). The highly conserved N- and C-terminal regions of UNC-53 (residues 11-143 and 164-1533), which together represent 95% of the protein, are (respectively) 35% and 24% identical (56% and 41% similar) to the corresponding regions of NAV2/RAINB1 (residues 90-213 and 941-2340). The human protein contains an additional ~720-residue sequence between these regions, not present in UNC-53.

The two proteins share several identifiable domains and motifs (Fig. 3B,C). There is a calponin homology (CH) domain in the N terminus, at amino acids 11 to 109. CH domains are present in various actin-binding proteins, including α-actinin and dystrophin, proteins known to crosslink actin filaments into bundles and networks. They share an additional putative actin-binding site of the LKK consensus (Van Troys et al., 1999). Both UNC-53 and NAV2/RAINB1 have a second LKK consensus actin-binding site, although these are not in equivalent positions in the two proteins. The same is true for two polyproline rich sequences, potential SH3-binding domains (Yu et al., 1994), that in UNC-53 are found at residues 487-495 and 537-545. UNC-53 also shares with its three human homologues two regions (890-923 and 1078-1113) predicted to adopt a coiled-coil configuration that could mediate homomeric or heteromeric protein-protein interactions (Maes et al., 2002), together with a nucleotide (NTP)-binding site contained within an ATPases-associated with diverse cellular activities (AAA) domain. Despite extensive sequence conservation, the members of the AAA family are implicated in diverse cellular functions, including cell cycle regulation and vesicle-mediated transport (Confalonieri and Duguet, 1995).

### *unc-53* expression pattern

The expression pattern of *unc-53* was characterised using several GFP reporter fusions (Fig. 3A). A region 2.3 kb upstream of the most 5′ SL1 splice site produced weak GFP expression in half a dozen unidentified neurones in the head. As this expression appeared not to correlate with the different *unc-53* phenotypes, other regions of the gene were assayed for their ability to drive GFP expression. We focused on the proximal part of phage S4 (Fig. 3A), as this clone was able to rescue partially the Unc and Egl phenotypes of *unc-53(n152)*, indicating that it contains regulatory elements necessary for the correct expression of UNC-53. When the first 6.2 kb of the S4 clone was used, in the pAB::GFP fusion, expression was seen in some pioneering neurones of the nerve ring, beginning at the early comma stage (Fig. 4A,B). At the two-fold stage, expression was detected in

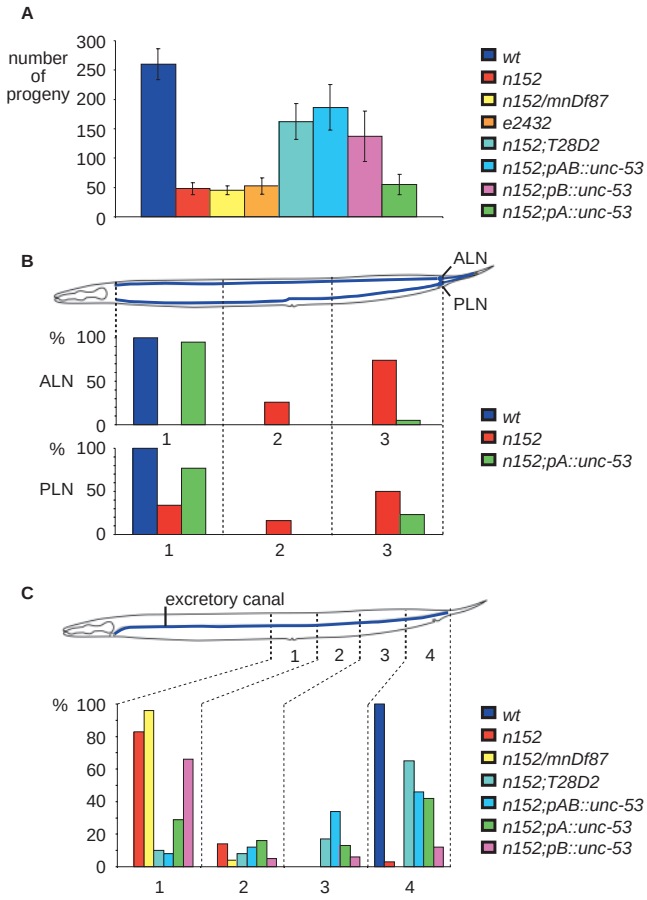


**Fig. 5.** Phenotypes of *unc-53* and their promoter-specific rescue. (A) The Egl phenotype was scored by counting the number of progeny from individual worms of different genotypes and is represented as an average with standard deviation for each strain. For wild-type, *n152* and *e2432* homozygous, and *n152/mnDf87* heterozygous worms, the progeny from 16, 29, 20 and 23 individual worms, respectively, were counted. Transgenic strains, all in an *unc-53(n152)* background, containing the cosmid T28D2 or the *unc-53* minigene expressed under the control of the AB, A or B promoter are represented as *n152;T28D2*, *n152;*pAB::*unc-53*, *n152;*pA::*unc-53* and *n152;*pB::*unc-53*, respectively. For each of these, the progeny of 12, 23, 23 and 19 individuals from two, five, two and five independent strains, respectively, were counted. Each independent strain of a given genotype gave similar results. Both *unc-53* alleles show a strong Egl phenotype, indistinguishable from that of *n152/mnDf87* heterozygotes. The *unc-53*(*n152*) phenotype was largely rescued by the cosmid T28D2, by pAB::*unc-53* and by pB::*unc-53*, but not by pA::*unc-53*. (B) Quantification of ALN and PLN axonal outgrowth defects. The worm was divided into three regions (1-3) with reference to the vulva and the anus. The stop point of ALN axons was determined using a pA::GFP reporter carried by wild-type (*n*=100), *n152* homozygous (*n*=50) and two independent strains of *n152;*pA::*unc-53* (*n*=100) worms. The percentage of axons stopping at each of the three positions was then calculated. The PLN defect was scored similarly for 70, 44 and 80 worms, respectively. The two *n152;*pA::*unc-53* strains gave comparable results. The *unc-53*(*n152*) phenotype was largely rescued by pA::*unc-53*.
(C) Quantification of the excretory canal outgrowth defect. The worm was divided into four regions (1-4) between the vulva and the anus. The stop point of canals was determined by DIC microscopy for wild type (*n*=100), *n152* (*n*=100), *n152/mnDf87* (*n*=52), *n152;T28D2* (*n*=48), *n152;*pAB::*unc-53* (*n*=50), *n152;*pA::*unc-53* (*n*=62) and *n152;*pB::*unc-53* (*n*=57). For the transgenic strains, two independent lines for each were examined. The percentage of canals stopping at each of the four positions was then calculated. *unc-53(n152)* was associated with a stereotyped arrest of the canal at the level of the vulva, that was almost as penetrant as *n152/mnDf87* heterozygotes. The phenotype was largely rescued by the cosmid T28D2. The pAB*::unc-53* and pA::*unc-53* constructs gave a degree of rescue, in contrast to pB::*unc-53*.

some 10 neurones in the head that extend axons into the nerve ring, and in two neurones in the tail that extend processes anteriorly. This expression pattern was confirmed by immunohistochemistry with MAb 16-48-2 (results not shown). At the three-fold stage, expression was seen in all DA motoneurones and persisted while they pioneered the dorsal nerve chord (Fig. 4C-F). It was also seen in four to six neurones in each of the four head ganglia, including ALA and RID in the dorsal ganglion, and four of the six neurones of the terminal bulb, including M5. In the tail, two neurones in the pre-anal ganglion and six in the lumbar ganglion, including PVQL and PVQR, showed pAB::GFP expression. Additionally, a transient expression was seen in the four rows of bodywall muscle cells in the embryo. After hatching, in L1 larvae, the expression domain extended to amphid and phasmid socket cells (Fig. 4G-I), and subsequently in L2 larvae to all the newly born AS motoneurones. In hermaphrodite L3 larvae, expression was seen in the sex myoblasts subsequent to their anterior migration towards the position of the presumptive vulva, and in adult worms at a high level in the vulval muscles vm1 and vm2 (Fig. 4J). In males, expression was seen in the diagonal (Fig. 4K) and spicule retractor muscles (Fig. 4L). Significantly, these are the only two muscle types in the male tail to be affected in the *unc-53* mutant. Additional cells expressing the pAB::GFP construct and presenting a phenotype in *unc-53* mutants are shown in Table 1. Although the mechanosensory neurones are affected in the *unc-53* mutant, they did not show expression of the pAB::GFP construct. It is therefore possible that there is an additional uncharacterised promotor upstream of the most 5′ SL1 trans-splice site. Putative expression of *unc-53* in the mechanosensory neurones could not be confirmed with the Mab 16-48-2 antibody, as we were unable to obtain staining in larvae or adults.

The existence of two transcripts with different SL1 spliced 5′ ends in the region covered by pAB::GFP suggested a bipartite nature for the *unc-53* promoter (Fig. 3A). Consequently, two non-overlapping reporter constructs, pA::GFP and pB::GFP were produced. These were associated with non-overlapping expression domains, that together recapitulated the expression pattern of pAB::GFP (Table1).

### *unc-53* act cell autonomously

As *unc-53* is expressed in cells that present a mutant phenotype in *unc-53* animals, the gene might be supposed to act in a cell-autonomous fashion. To test this hypothesis, we constructed mini genes that contained the cell-specific promoters pA or pB, or the combined pAB fused to an *unc-53* cDNA. Although the combined pAB promoter construct rescued the Egl and the excretory canal extension phenotype of *n152* at levels comparable with the rescue obtained with cosmid T28D2, when the promoters were tested individually, differential rescue of phenotypes was observed (Fig. 5). The pB::*unc-53* fusion, that is expressed in the sex muscles, showed the same level of rescue

of the Egl phenotype as pAB::*unc-53*. At a cellular level, this rescue was associated with a restoration of wild-type morphology and attachment of the sex muscles (results not shown). By sharp contrast, the pA::*unc-53* fusion, which is not expressed in the sex muscles, failed to rescue the Egl phenotype (Fig. 5A). However, the pA promoter does drive expression in the ALN and PLN neurones, and the pA::*unc-53* fusion gave a high degree of rescue of their extension phenotypes in *n152* (Fig. 5B). Furthermore, while pB was not associated with expression in the excretory cell, pA was occasionally, and only pA::*unc-53* produced some rescue of excretory canal extension (Fig. 5C).

### Overexpression of *unc-53* in bodywall muscles leads to overgrowth

The body wall muscles of *C. elegans* are arranged longitudinally in four quadrants along the anteroposterior axis. In wild-type animals, body muscle cells are normally spindle shaped, while in *unc-53(e2432)* animals, these cells sometimes have reduced processes and fork-shaped tips (T. B., unpublished). Transient expression of *unc-53* in embryonic body wall muscles was observed with the pAB::GFP reporter. No significant signal was detected using the anti-UNC-53 monoclonal antibody, however, suggesting that the endogenous level of UNC-53 is very low in these cells. To investigate further the role of *unc-53*, we tested the effect of its overexpression in the body wall muscles by expressing the *unc-53* cDNA under the control of the *unc-54* promoter (p*unc-54::unc-53*). The *unc-54* gene, which encodes the myosin heavy chain, is transcribed in body muscle from the comma stage onwards (Okkema et al., 1993). In comparison with wild-type growth cones, revealed by a p*unc-54*::GFP reporter (Fig. 6A,C), the processes of p*unc-54::unc-53* embryos were overextended along the anteroposterior axis of the animal (Fig. 6B,D). The growth cones of *punc-54::unc-53*-expressing cells were on average 54% longer than the length of the growth cones of wild-type muscle cells in late embryos (Table 2). In addition, a variably penetrant lethality was observed, associated with severe morphological defects and detachment of muscle cells from the hypodermis (Fig. 6F; Table 2).

### Interaction of UNC-53 with SEM-5/GRB2

The observation that certain alleles of *unc-53* enhance the sex myoblast migration defect seen in *sem-5* mutants suggests that UNC-53 and SEM-5 co-operate to regulate sex myoblast migration (Chen et al., 1997). SEM-5 contains SH2 and SH3 domains, while UNC-53 contains putative SH3-binding domains, suggesting that this co-operation might be mediated through a direct molecular interaction. To investigate this possibility, we first produced an almost full-length $^{35}$S-labelled form of UNC-53 (UNC-53Δ71C) in vitro (Fig. 7A). We then tested the interaction between UNC-53Δ71C and SEM-5 in a GST pull-down assay. The in vitro translated radiolabelled UNC-53Δ71C was incubated with beads coupled to GST or to GST-SEM-5. UNC-53Δ71C was found to associate specifically with SEM-5, but did not bind to a significant extent to GST alone (Fig. 7B).

It has been shown that human GRB2 can rescue the sex myoblast migration defects of *sem-5* mutants and as such can be considered a true orthologue (Stern et al., 1993). We therefore tested whether UNC-53Δ71C and GRB2 interact directly. UNC-53Δ71C produced in bacteria was used in western blot overlays, revealed with biotinylated GST or GST-GRB2 (Fig. 7C). A specific interaction with GRB2 was observed. Interestingly, no signal was detectable with an UNC-53 fusion protein containing the last 541 amino acids, thus lacking the polyproline repeats (data not shown). This provides supportive evidence that these could directly bind to the SH3 domains of a SEM-5/GRB2 adapter protein.

**Table 2. Effect of *unc-53* overexpression on the length of muscle cell growth cones**

| | Length of growth cone (μm)* | | |
|---|---|---|---|
| Transgenic strain† | Early elongation‡ | Late elongation§ | Lethality (%)¶ |
| p*unc-54*::GFP | 5.5±1.3 (19) | 6.8±1.3 (36) | 0 (178) |
| p*unc-54::unc-53* | 8.1±2.1 (32) | 10.5±3.8 (35) | 60 (115) |

*The average distance (±s.d.) from the periphery of the nucleus to the growth cone tip is shown. The number of cells scored is given in brackets, one to three cells were measured in a given embryo. The figures for the two transgenic strains are significantly different using a two sample *t*-test ($P$=0.01).

†Three p*unc-54::unc-53* and two p*unc-54*::GFP lines were examined. Data for one representative line is shown for each construct.

‡Early elongation refers to embryos at the comma to 1.5-fold stage.

§Late elongation refers to embryos at the three-fold stage.

¶Lethality refers to the percentage of transgenic eggs that did not hatch or which hatched but died early in L1. The number of transgenic progeny scored is given in brackets.

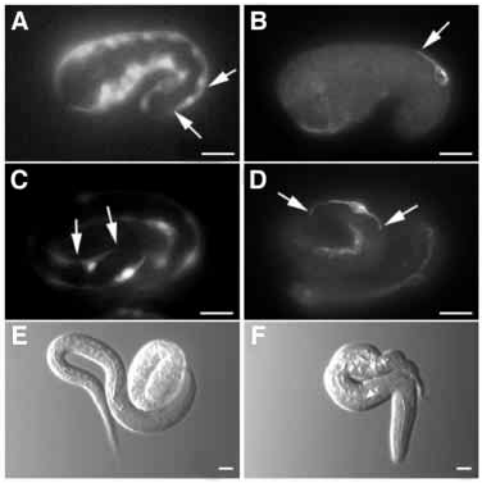


**Fig. 6.** Overexpression of *unc-53* in muscle cells. In body wall muscle cells, overexpression of *unc-53* results in over-extension along the longitudinal axis. (A,C) Wild-type body wall muscle cells visualised with the p*unc-54*::GFP reporter pPD93.48, at the comma (A) and three-fold (C) stages. (B,D) Transgenic embryos carrying the construct p*unc-54::unc-53* (pTB113) immunostained with the anti-UNC-53 monoclonal antibody MAb 16-48-2 at the comma (B) and three-fold stages (D). Arrows mark cell extremities. (E) Wild-type p*unc-54*::GFP L1 larva and three-fold embryo visualised with DIC optics. (F) Mutant p*unc-54::unc-53* L1 larva showing severe morphological defects in the posterior body. Scale bars: 10 μm.

## DISCUSSION

### UNC-53 affects many cell and axon migrations in *C. elegans*

The gene *unc-53* is required for cell migrations and the

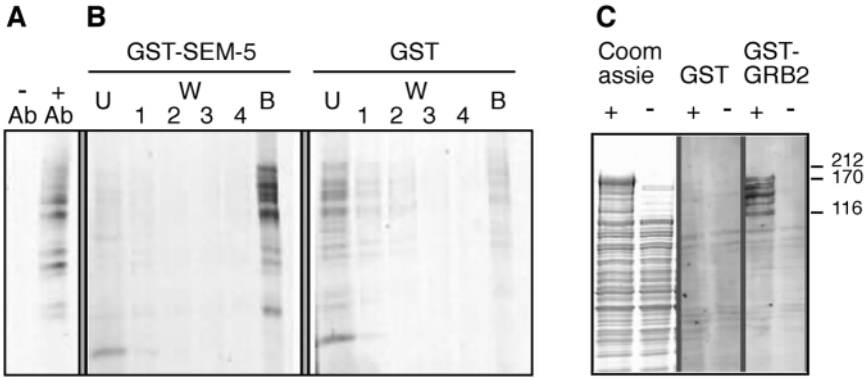


**Fig. 7.** UNC-53 binds SEM-5/GRB2. (A) Immunoprecipitation of in vitro produced UNC-53. Radiolabelled UNC-53Δ71C protein, transcribed and translated in vitro, was immunoprecipitated with the MAb 16-48-2 under denaturing conditions, then incubated with protein G sepharose. The beads were washed and the bound products analysed by SDS-PAGE and fluorography (lane + Ab). As a control (lane – Ab), a reaction without MAb 16-48-2 was treated identically. The lower bands most likely correspond to proteins initiated at internal methionines, or arising from premature termination or proteolytic degradation. (B) GST pull-down assays. The radiolabelled UNC-53Δ71C protein was incubated with SEM-5-GST (left panel) or GST (right panel) coupled to sepharose beads. After four washes, the remaining proteins bound to the beads were analysed by SDS-PAGE and fluorography. U, unbound; W1-4, washes 1 to 4; B, bound protein. (C) Western blot overlay assays. Cell lysates from bacteria containing the UNC-53Δ71C-encoding plasmid pTB61, from induced (+) or uninduced (–) cultures were denatured in Laemmli buffer and the proteins separated by 5-25% gradient SDS-PAGE. Total proteins were revealed by Coomassie Blue staining (left panel). Additional gels were blotted to nylon membrane, incubated with biotinylated GST (middle panel) or biotinylated GST-GRB2 protein (right panel), and bound protein complexes subsequently detected using an alkaline phosphatase-linked anti-streptavidin-antibody and chromogenic substrate. The positions of the molecular weight markers (in kDa) are shown.

outgrowth of cellular processes, predominantly along the AP axis. *unc-53* is capable of acting in a fasciculation-independent manner in pioneering neurones, including PLM (Hekimi and Kershaw, 1993) and in ALN during its extension from the tail to mid-body region. In the absence of *unc-53*, not only does ALN arrest its growth prematurely, but it also sends projections to the dorsal cord, in stark contrast to wild type ALN axons, which never stray from their AP path. In some cases, mutant axons arriving at the dorsal cord, then turn back and extend towards the tail. Furthermore, *unc-53* appears to be required only in last half of the trajectory of the excretory canals from the mid-body region to the tail. These results argue against an involvement of *unc-53* in the general mechanisms of cell migration, but rather suggests that *unc-53* is a key component of the AP guidance system in the cells in which it is expressed.

*unc-53*::GFP is expressed in most neurones and migrating cells known to be affected in *unc-53* mutants. Furthermore, the timing of *unc-53* expression in most of these cells is coincident with the movement of these cells or the outgrowth of their axons. The expression of *unc-53* in specific cells, including the sex muscles, the excretory cell or the ALN neurones was sufficient to rescue their associated cellular phenotypes. Moreover, overexpression of *unc-53* in body wall muscles leads to exaggerated outgrowth. Wild-type muscle cells possess a remarkable plasticity during morphogenesis, which allows them to fill the space created by ablation of embryonic muscle blastomeres (Moerman et al., 1996). However, even these extended wild-type cells retain their characteristic spindle shape and are not as long as the p*unc-54::unc-53* cells observed in the present study. In addition, while detachment of p*unc-54::unc-53* overexpressing cells from the hypodermis sometimes occurs, the long tendril-like growth cone extensions observed in these cells (Fig. 6D) are not seen in known muscle detachment mutants (D. Moerman, personal communication). This provides evidence in support of a cell-autonomous function of UNC-53 in cell migration and axon guidance.

The excretory canal and ALA send posteriorly directed processes along adjacent trajectories (White et al., 1986). In *unc-53*, the observed stereotyped mid-body arrest of the excretory canal is highly reminiscent of the premature arrest of ALA in the *ceh-17* mutant (Pujol et al., 2000). The fact that ALA is wild type in *unc-53* mutants and, conversely, that the excretory canal is normal in the *ceh-17* mutant, would tend to indicate that the growth of these two cellular processes is mutually independent. These results do, however, raise the possibility that they are controlled partially by the same guidance cues, localised to the mid-body. Analysis of sex myoblast migration in this region has revealed a complex interaction of gonad-dependent and -independent signals. Significantly, *unc-53* is required for the gonad-independent attraction of the sex myoblasts to the mid-body (Chen et al., 1997). We have demonstrated a further role for *unc-53* in the final longitudinal migrations of the sex myoblasts away from the vulva that accompany their division. This clearly suggests that *unc-53* is involved in the response to as yet unidentified directional cues that originate from the mid-body.

## UNC-53 homology domains could link SEM-5 and the actin cytoskeleton

Molecular analyses revealed multiple *unc-53* transcripts. The longest encodes a predicted protein of 1583 amino acids containing a CH domain, two LKK motifs, two SH3-binding domain, two coiled-coil regions and a nucleotide-binding domain. Sequence analysis of two *unc-53* alleles, *n152* and *e2432* showed that they probably correspond to severely truncated proteins, lacking the conserved nucleotide binding domain, the C-terminal LKK motif and the two coiled-coil regions. These modules are therefore likely to be functionally important. As the regions associated with a putative function make up only about 25% of the protein, molecular analysis of additional mutations may pinpoint further domains involved in specific molecular interactions.

Genetic evidence has suggested that *sem-5* and *unc-53* co-operate to control sex myoblast migration (Chen et al., 1997). SEM-5 is the *C. elegans* GRB2 homologue and consists exclusively of SH2 and SH3 domains (Clark et al., 1992). The biochemical experiments of the present study suggest that the

interaction between *unc-53* and *sem-5* is direct. UNC-53 protein physically associates with SEM-5 and its mammalian homologue GRB2 in vitro, presumably via its SH3-binding domain.

Although functional actin-binding modules cannot always be accurately predicted, UNC-53 does contain conserved a CH domain and LKK motifs (Van Troys et al., 1999). The first is found in a variety of cytoskeletal and signal transduction molecules implicated in the regulation of cell shape dynamics (Stradal et al., 1998). The actin cross-linking proteins α-actinin, β-spectrin and dystrophin each contain two relatively dissimilar CH domains (Carugo et al., 1997), while UNC-53, in common with Vav and calponin, contains only one. Preliminary experiments suggest that UNC-53 is able to co-sediment actin in vitro (E. S., unpublished). It is therefore possible that UNC-53 could link SEM-5 to the actin cytoskeleton.

### Models for UNC-53 activity

Studies in invertebrates and vertebrates have suggested that the leading edge of a migrating cell or the growth cone at the tip of an axon are steered in a similar manner by attractive and repulsive extracellular cues, which may be emitted along multiple axes. In the growth cone, cell-surface receptors receive specific and competing signals and transduce them to components within the cell. This leads to changes in the cytoskeletal architecture resulting in the localised accumulation of polymerised actin in the growth cone. Subsequent translocation of microtubules to this point drives the growth cone forward stepwise in that chosen direction (Bentley and O'Connor, 1994).

In this context, two models for the action of UNC-53 can be proposed. Within the cell, activation of UNC-53 by SEM-5 could lead to the recruitment of UNC-53 to the actin cytoskeleton and then regulate, perhaps via nucleotide binding, the crosslinking of actin molecules to stabilise a growth cone spike and promote extension in a specific direction. Alternatively, UNC-53 may act as a signal relay, associated with the cytoskeleton, but not directly responsible for the modifications of the actin cytoskeleton associated with growth cone extension. In both models, the *unc-53* pathway integrates signals received at the cell surface and determines the direction and rate of growth cone extension. Preliminary experiments have suggested that UNC-53 does indeed localise to the cytoskeleton. Further characterisation of the interactions between UNC-53 and its molecular partners may shed more light on the mechanisms of cell migration and growth cone extension.

We thank J. Ewbank for precious help with the writing; R. Horvitz, E. Hedgecock, A. Chisholm and the *Caenorhabditis* Genetics Center (funded by the NIH National Center for Research Resources) for mutant strains; M. Stern for the GST-SEM-5 and GST-GRB2 fusions; A. Fire for pPD93.48 and nematode expression vectors; P. Y. Goh, I. Maillet, I. Roelens and C. Couillault for their contribution to the work; M. A. Felix for vulval cell identification; C. Buesa for communicating results before publication, D. Moerman for helpful discussions; and Y. Jin and anonymous reviewers for critical comments on the manuscript. This work was supported by grants to J. V. from the European Community and the Concerted Research Actions (GOA) of Ghent University. E. S. gratefully acknowledges the support of a long-term EMBO fellowship. Part of this study was supported by the Natural Sciences and Engineering Research Council of Canada (E. S.) and Assedic (N. P.).

## REFERENCES

**Ausubel, F. M., Brent, R., Kingston, R. E., Moore, D. D., Seidmand, J. G., Smith, J. A. and Struhl, K.** (1993). *Current Protocols in Molecular Biology*. New York: J. Wiley & Sons.

**Bentley, D. and O'Connor, T. P.** (1994). Cytoskeletal events in growth cone steering. *Curr. Opin. Neurobiol.* **4**, 43-48.

**Branda, C. S. and Stern, M. J.** (2000). Mechanisms controlling sex myoblast migration in *Caenorhabditis elegans* hermaphrodites. *Dev. Biol.* **226**, 137-151.

**Brenner, S.** (1974). The genetics of *Caenorhabditis elegans*. *Genetics* **77**, 71-94.

**Carugo, K. D., Banuelos, S. and Saraste, M.** (1997). Crystal structure of a calponin homology domain. *Nat. Struct. Biol.* **4**, 175-179.

**Chen, E. B., Branda, C. S. and Stern, M. J.** (1997). Genetic enhancers of *sem-5* define components of the gonad-independent guidance mechanism controlling sex myoblast migration in *Caenorhabditis elegans* hermaphrodites. *Dev. Biol.* **182**, 88-100.

**Chisholm, A. and Tessier-Lavigne, M.** (1999). Conservation and divergence of axon guidance mechanisms. *Curr. Opin. Neurobiol.* **9**, 603-615.

**Clark, S. G., Stern, M. J. and Horvitz, H. R.** (1992). *C. elegans* cell-signalling gene *sem-5* encodes a protein with SH2 and SH3 domains. *Nature* **356**, 340-344.

**Confalonieri, F. and Duguet, M.** (1995). A 200-amino acid ATPase module in search of a basic fuction. *BioEssays* **17**, 639-650.

**Goh, P. Y. and Bogaert, T.** (1991). Positioning and maintenance of embryonic body wall muscle attachments in *C. elegans* requires the *mup-1* gene. *Development* **111**, 667-681.

**Hao, J. C., Yu, T. W., Fujisawa, K., Culotti, J. G., Gengyo-Ando, K., Mitani, S., Moulder, G., Barstead, R., Tessier-Lavigne, M. and Bargmann, C. I.** (2001). *C. elegans* Slit acts in midline, dorsal-ventral, and anterior-posterior guidance via the SAX-3/Robo Receptor. *Neuron* **32**, 25-38.

**Hedgecock, E. M., Culotti, J. G., Hall, D. H. and Stern, B. D.** (1987). Genetics of cell and axon migrations in *Caenorhabditis elegans*. *Development* **100**, 365-382.

**Hedgecock, E. M. and Norris, C. R.** (1997). Netrins evoke mixed reactions in motile cells. *Trends Genet.* **13**, 251-253.

**Hekimi, S. and Kershaw, D.** (1993). Axonal guidance defects in a *Caenorhabditis elegans* mutant reveal cell- extrinsic determinants of neuronal morphology. *J. Neurosci.* **13**, 4254-4271.

**Hodgkin, J.** (1983). Male phenoypes and mating efficiency in *Caenorhabditis elegans*. *Genetics* **103**, 43-64.

**Krause, M. and Hirsh, D.** (1987). A trans-spliced leader sequence on actin mRNA in *C. elegans*. *Cell* **49**, 753-761.

**Li, W., Herman, R. K. and Shaw, J. E.** (1992). Analysis of the *Caenorhabditis elegans* axonal guidance and outgrowth gene *unc-33*. *Genetics* **132**, 675-689.

**Lin, M. Z. and Greenberg, M. E.** (2000). Orchestral maneuvers in the axon: trio and the control of axon guidance. *Cell* **101**, 239-242.

**Lowenstein, E. J., Daly, R. J., Batzer, A. G., Li, W., Margolis, B., Lammers, R., Ullrich, A., Skolnik, E. Y., Bar-Sagi, D. and Schlessinger, J.** (1992). The SH2 and SH3 domain-containing protein GRB2 links receptor tyrosine kinases to ras signaling. *Cell* **70**, 431-442.

**Maes, T., Barcelo, A. and Buesa, C.** (2002). Neuron NAVs: a human gene family with homology to *unc-53*, a cell guidance gene of *C. elegans*. *Genomics* (in press).

**McIntire, S. L., Garriga, G., White, J., Jacobson, D. and Horvitz, H. R.** (1992). Genes necessary for directed axonal elongation or fasciculation in *C. elegans*. *Neuron* **8**, 307-322.

**McLeod, M., Stein, M. and Beach, D.** (1987). The product of the mei3+ gene, expressed under control of the mating- type locus, induces meiosis and sporulation in fission yeast. *EMBO J.* **6**, 729-736.

**Mello, C. C., Kramer, J. M., Stinchcomb, D. and Ambros, V.** (1991). Efficient gene transfer in *C. elegans*: extrachromosomal maintenance and integration of transforming sequences. *EMBO J.* **10**, 3959-3970.

**Merrill, R. A., Plum, L. A., Kaiser, M. E. and Clagett-Dame, M.** (2002). A mammalian homolog of unc-53 is regulated by all-trans retinoic acid in neuroblastoma cells and embryos. *Proc. Natl. Acad. Sci. USA* **99**, 3422-3427.

**Moerman, D. G., Hutter, H., Mullen, G. P. and Schnabel, R.** (1996). Cell autonomous expression of perlecan and plasticity of cell shape in embryonic muscle of *Caenorhabditis elegans*. *Dev. Biol.* **173**, 228-242.

**Nelson, F. K., Albert, P. S. and Riddle, D. L.** (1983). Fine structure of the *Caenorhabditis elegans* secretory-excretory system. *J. Ultrastruct. Res.* **82**, 156-171.

**Ogura, K., Shirakawa, M., Barnes, T. M., Hekimi, S. and Ohshima, Y.** (1997). The UNC-14 protein required for axonal elongation and guidance in *Caenorhabditis elegans* interacts with the serine/threonine kinase UNC-51. *Genes Dev.* **11**, 1801-1811.

**Okkema, P. G., Harrison, S. W., Plunger, V., Aryana, A. and Fire, A.** (1993). Sequence requirements for myosin gene expression and regulation in *Caenorhabditis elegans*. *Genetics* **135**, 385-404.

**Otsuka, A. J., Franco, R., Yang, B., Shim, K. H., Tang, L. Z., Zhang, Y. Y., Boontrakulpoontawee, P., Jeyaprakash, A., Hedgecock, E., Wheaton, V. I. et al. (**1995). An ankyrin-related gene (*unc-44*) is necessary for proper axonal guidance in *Caenorhabditis elegans*. *J. Cell Biol.* **129**, 1081-1092.

**Pujol, N., Torregrossa, P., Ewbank, J. J. and Brunet, J. F.** (2000). The homeodomain protein CePHOX2/CEH-17 controls antero-posterior axonal growth in *C. elegans*. *Development* **127**, 3361-3371.

**Siddiqui, S. S.** (1990). Mutations affecting axonal growth and guidance of motor neurons and mechanosensory neurons in the nematode *Caenorhabditis elegans*. *Neurosci. Res.* **13**, S171-S190.

**Stern, M. J., Marengere, L. E., Daly, R. J., Lowenstein, E. J., Kokel, M., Batzer, A., Olivier, P., Pawson, T. and Schlessinger, J.** (1993). The human GRB2 and Drosophila Drk genes can functionally replace the *Caenorhabditis elegans* cell signaling gene *sem-5*. *Mol. Biol. Cell* **4**, 1175-1188.

**Steven, R., Kubiseski, T. J., Zheng, H., Kulkarni, S., Mancillas, J., Ruiz Morales, A., Hogue, C. W., Pawson, T. and Culotti, J.** (1998). UNC-73 activates the Rac GTPase and is required for cell and growth cone migrations in *C. elegans*. *Cell* **92**, 785-795.

**Stradal, T., Kranewitter, W., Winder, S. J. and Gimona, M.** (1998). CH domains revisited. *FEBS Lett.* **431**, 134-137.

**Sulston, J. E. and Horvitz, H. R.** (1977). Post-embryonic cell lineages of the nematode, *Caenorhabditis elegans*. *Dev. Biol.* **56**, 110-156.

**Sulston, J. E. and Horvitz, H. R.** (1981). Abnormal cell lineages in mutants of the nematode *Caenorhabditis elegans*. *Dev. Biol.* **82**, 41-55.

**Sulston, J. E., Albertson, D. G. and Thomson, J. N.** (1980). The *Caenorhabditis elegans* male: postembryonic development of nongonadal structures. *Dev. Biol.* **78**, 542-576.

**Tessier-Lavigne, M. and Goodman, C. S.** (1996). The molecular biology of axon guidance. *Science* **274**, 1123-1133.

**Trent, C., Tsung, N. and Horvitz, H. R.** (1983). Egg-laying defective mutants of the nematode of *C. elegans*. *Genetics* **104**, 619-647.

**Van Troys, M., Vandekerckhove, J. and Ampe, C.** (1999). Structural modules in actin-binding proteins: towards a new classification. *Biochim. Biophys. Acta* **1448**, 323-348.

**White, J. G., Southgate, E., Thomson, J. N. and Brenner, S.** (1986). The structure of the nervous system of the nematode *C. elegans*. *Philos. Trans. R. Soc. Lond. B Biol. Sci.* **314B**, 1-340.

**Wightman, B., Baran, R. and Garriga, G.** (1997). Genes that guide growth cones along the *C. elegans* ventral nerve cord. *Development* **124**, 2571-2580.

**Yu, H., Chen, J. K., Feng, S., Dalgarno, D. C., Brauer, A. W. and Schreiber, S. L.** (1994). Structural basis for the binding of proline-rich peptides to SH3 domains. *Cell* **76**, 933-945.